Bass Strait Forcing of Coastal Trapped Waves: ACE Revisited

R. A. MORROW AND IAN S. F. JONES

Marine Studies Centre, University of Sydney. N.S.W., Australia

R. L. SMITH AND P. J. STABENO

College of Oceanography, Oregon State University, Corvallis, Oregon

24 August 1989 and 13 February 1990

1. Introduction

Historically, the east coast of Australia has been important in the study of coastal trapped waves (CTW). Hamon (1962, 1963, 1966) found that perturbations in sea level, adjusted for atmospheric pressure, propagate northward along the east Australian coast. This was the first observation of "continental shelf waves", now termed coastal trapped waves. In 1983/84, the Australian Coastal Experiment (ACE) was conducted off the southeast Australian coast to compare observation and theory of low-frequency coastal trapped waves (Freeland et al. 1986; Church et al. 1986a,b).

In planning ACE and in the theoretical study by Clarke and Thompson (1984), it was assumed that the coastal trapped waves would be forced by local winds in the region between Cape Howe and Sydney (Fig. 1). Instead, the coastal trapped waves were found to be fully developed when entering the southern end of the ACE region and propagate northward through the region as free waves (Freeland et al. 1986). Little coastal trapped wave energy was detected off eastern Tasmania, which suggests that CTWs did not propagate around the southern tip of Tasmania and then north across the eastern escarpment of Bass Strait.

Since the observations indicate neither local generation nor propagation around Tasmania, the alternatives are that the CTW energy is either generated in or propagates through Bass Strait. Church and Freeland (1987) suggested the ACE coastal trapped wave energy may be generated in the Great Australian Bight, and propagate in some form through Bass Strait and then into the southern ACE array. The observed sea level (adjusted for atmospheric pressure) and atmospheric pressure propagates eastward at 10 m s^{-1} across the Great Australian Bight, although the sea level fluctuations propagate at 15 m s^{-1} between the western and eastern ends of Bass Strait.

However there is no established mechanism for the transfer of energy through Bass Strait at 15 m s^{-1}. Theoretically, this energy could propagate through Bass Strait as a barotropic Kelvin wave and an infinite set of CTWs, which would exist due to stratification and the narrow "shelf" near the northern coast. Clarke (1987) shows that only the Kelvin wave is of practical importance since the CTWs are rapidly damped out by friction on alongshore scales of 40 km or less. The barotropic Kelvin wave has a phase speed of $\sqrt{gh}$, so along Bass Strait (average depth of 80 m) the phase speed is 28 m s^{-1}, much faster than the 15 m s^{-1} observed by Church and Freeland (1987).

There is some question as to how much energy would enter Bass Strait from the western side. Clarke (1987) has shown that most of the CTW energy incident on the western end of Bass Strait would propagate south as escarpment waves. Sea level measurements from the west of Tasmania are sparse (Church and Freeland 1987) but results indicate that some energy is propagating south, although it does not continue around to the eastern coast.

The direct wind forcing within Bass Strait was examined by Freeland et al. (1986). They applied an analytic solution for the wind forced motion in Bass Strait following Gill and Clarke (1974). Their model yielded a greater energy flux than that observed at Cape Howe and highlighted the importance of wind forcing over Bass Strait as a possible source of the energy flux. Freeland et al. (1986) also investigated whether the wind stress over the 150 km of shelf between the eastern end of Bass Strait and Cape Howe would be sufficient to generate the observed energy flux at Cape Howe. Their calculated energy flux was only one-fifth of the measured flux.

Clarke (1987) has described an analytical model for low frequency wind-driven flow generated within Bass Strait, based on the general model of Clarke and Van Gorder (1986). His calculations show that the Bass Strait energy flux is consistent with the amount of energy entering the ACE region. Clarke (1987) used the standard deviation of wind stress measured at Gabo Island (Fig. 1) as the estimate of wind stress for the entire Bass Strait region. These winds may give unrealistic results, as they are not within the area modeled

Corresponding author address: Ms. R. A. Morrow, Marine Studies Centre, University of Sydney, N.S.W. 2006, Australia.

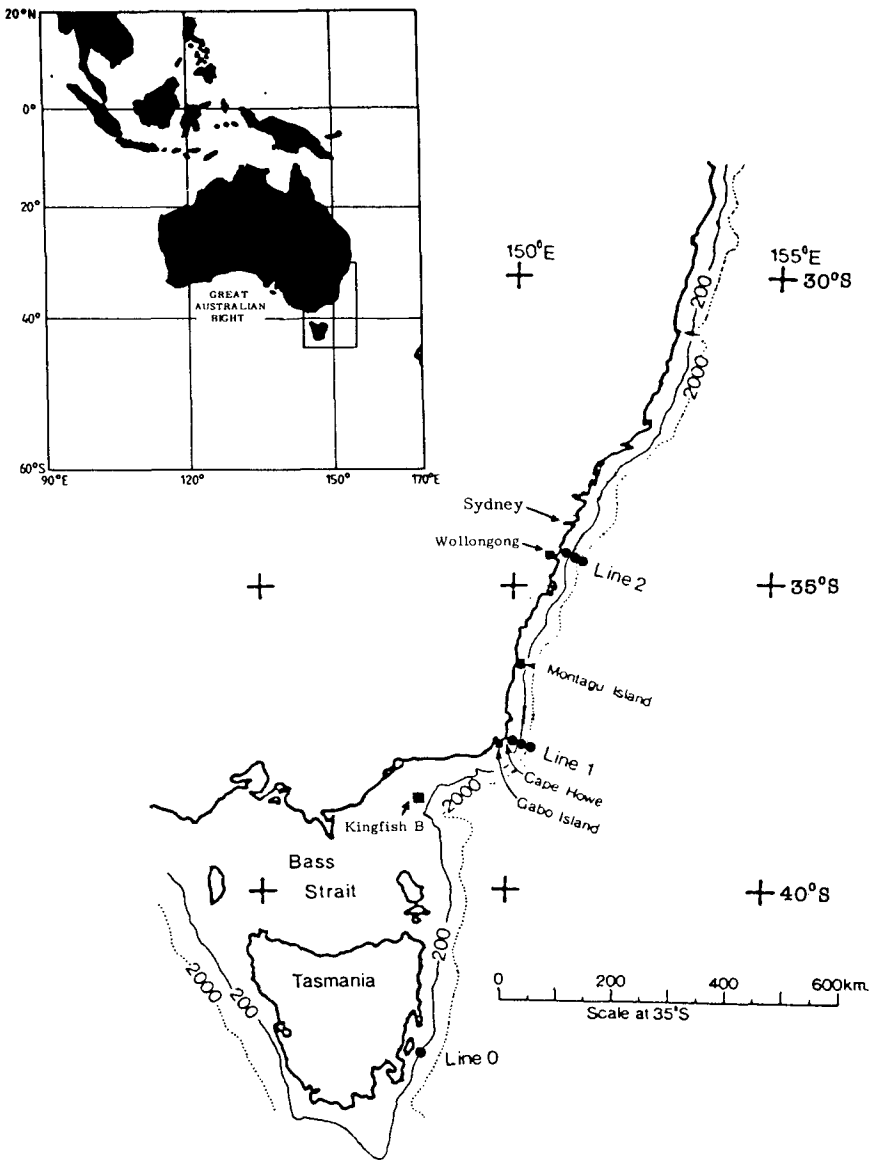

FIG. 1. Location of current meter moorings (solid dots) and meteorological stations (squares).

and are measured on a headland that induces topographic distortion.

We wish to examine the relationship between the low-frequency winds and currents in Bass Strait and on the east Australian coast, and highlight the important forcing relationships. We will apply high quality wind data, measured from the Kingfish B platform within Bass Strait, to the windforced Kelvin wave model (Clarke 1987). The resulting energy flux and Kelvin wave currents will be compared with the observed results. The process by which the Kelvin wave in Bass Strait is converted into coastal trapped waves at Line 1 is not addressed by Clarke (1987) but we can compare the energy fluxes in the two systems. Buchwald and Kachoyan (1987) have provided such an explanation by showing theoretically how currents in Bass Strait (wind-driven or otherwise) can force coastal trapped waves.

2. Data

The wind and current data are measured during the ACE period, from the ESSO/BHP Kingfish B (KFB) oil platform in eastern Bass Strait (Fig. 1). Since we are interested in the low frequency variability (coastal trapped waves with periods greater than 2–3 days), all the records have been low-pass filtered with a half-amplitude point of 40 hours, then decimated to yield semi-daily points that are consistent with the ACE data. The mean and standard deviation of each wind and current record are shown in Table 1.

TABLE 1. Means and standard deviations of low-passed 12-hourly alongshore time series of wind stress and current, for the period 31 October 1983 to 3 March 1984

	Mean	Standard deviation	Alongshore direction (°T)
	Wind stress (dyn cm^{-2})		
Kingfish B*	0.25	2.31	90°
Gabo Island (Line 1)	0.55	3.00	27°
Montagu Island	−0.12	1.27	13°
Wollongong (Line 2)	−0.01	0.49	26°
	Currents (cm s^{-1})		
Kingfish B	−5.5	11.9	45°
Line 0	3.3	15.7	20°
Line 1	3.1	29.7	20°
Line 2	−5.7	20.2	30°

* Adjusted from 65 m to 10 m level.

a. Meteorological data

Good quality wind data (17 minute averages, three per hour) were measured on the eastern end of Bass Strait at the ESSO/BHP Kingfish B (KFB) oil platform (38°36′S, 148°11′E). The platform is situated near the shelf break, approximately 80 km from the coast. A Synchrotrac wind speed and direction transmitter was positioned on a tower 65 m above mean sea level. The wind stress were calculated using the Large and Pond (1981) formula and reduced to the conventional 10 m level by assuming a logarithmic boundary layer (Wu 1980). The 10 m wind stress contained 85% of the variance of the stress calculated from the 65 m winds.

Wind data (Forbes 1987) were obtained from three of the shore-based meteorological stations used in the ACE Experiment: Gabo Island, Montague Island and Wollongong (Fig. 1). These three stations were the closest to the ACE current meter arrays. For this paper, each of the winds was rotated into principal axis coordinates (27°T, 13°T, 26°T respectively) and are nearly parallel to the local coastline orientation at each site. The wind stress data are the same as that used in the ACE analysis by Freeland et al. (1986). The wind data has not been reduced to the 10 m level before calculating the stress but rather the values at 15 m, 61 m and 19 m are used.

Figure 2 shows the filtered vector winds in Bass Strait and from the ACE Experiment. The series were plotted with their alongshore axes directed to the top of the page. The KFB winds were well correlated with the Line 1 winds (0.77) and Line 2 winds (0.67). All the wind records except KFB are shore-based and thus may have directional and speed biases induced by the topography.

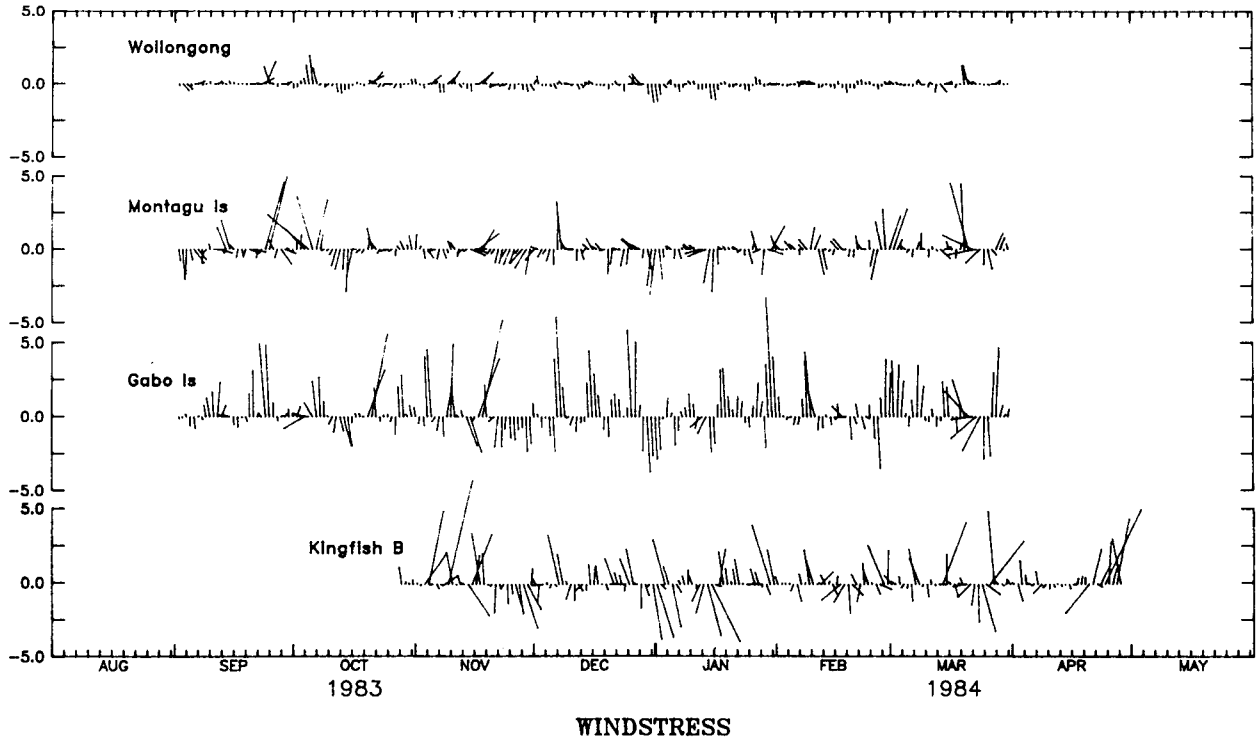

FIG. 2. Time series of low-passed wind stress vectors from Bass Strait and east Australian coast stations. Wind stress is measured in dyn cm^{-2}. Vectors have been rotated with the alongshore component directed toward the top of the page.

b. Current meter data

Currents were measured at KFB using three electromagnetic current meters, with depths at 7 m, 38 m and 69 m below mean sea level in a water depth of 78 m. Good current data were measured at the bottom current meter from October 1983 to April 1984, (the top and middle current meters were affected by sensor degradation). For comparison with the ACE data set (September 1983–March 1984) only the 69 m current record is presented. The current record has been rotated to its principal axis (45°T).

The ACE current records are from two lines of moorings across the continental shelf: Line 1 at 37.5°S at Cape Howe and Line 2 at 34.5°S near Sydney (Fig. 1). An additional mooring was deployed off the east coast of Tasmania: Line 0 at 42°S. The two principal lines were perpendicular to the local coastline. Current records from Lines 0, 1 and 2 were rotated into a local coordinate system, with alongshore component toward 20°T, 20°T and 30°T respectively. In general the principal axis orientation for the individual current records agrees well with this choice of coordinates (Huyer et al. 1988). In the case of the ACE current data, one representative series is chosen from each line, the choice being the midshelf record with the maximum length of series. The selected current records at Lines 0, 1 and 2 were at (125, 125, 132) m in (200, 140, 142) m water depth. All the ACE current meter data is presented in Freeland et al. (1985) and the detailed ACE current analysis is described in Freeland et al. (1986), and Huyer et al. (1988).

Figure 3 shows the filtered vector plots of the currents; currents at KFB are highly correlated with Line 1 (0.88) and Line 2 (0.60). The standard deviation at KFB (69 m depth) is less than at Line 1 (125 m depth)

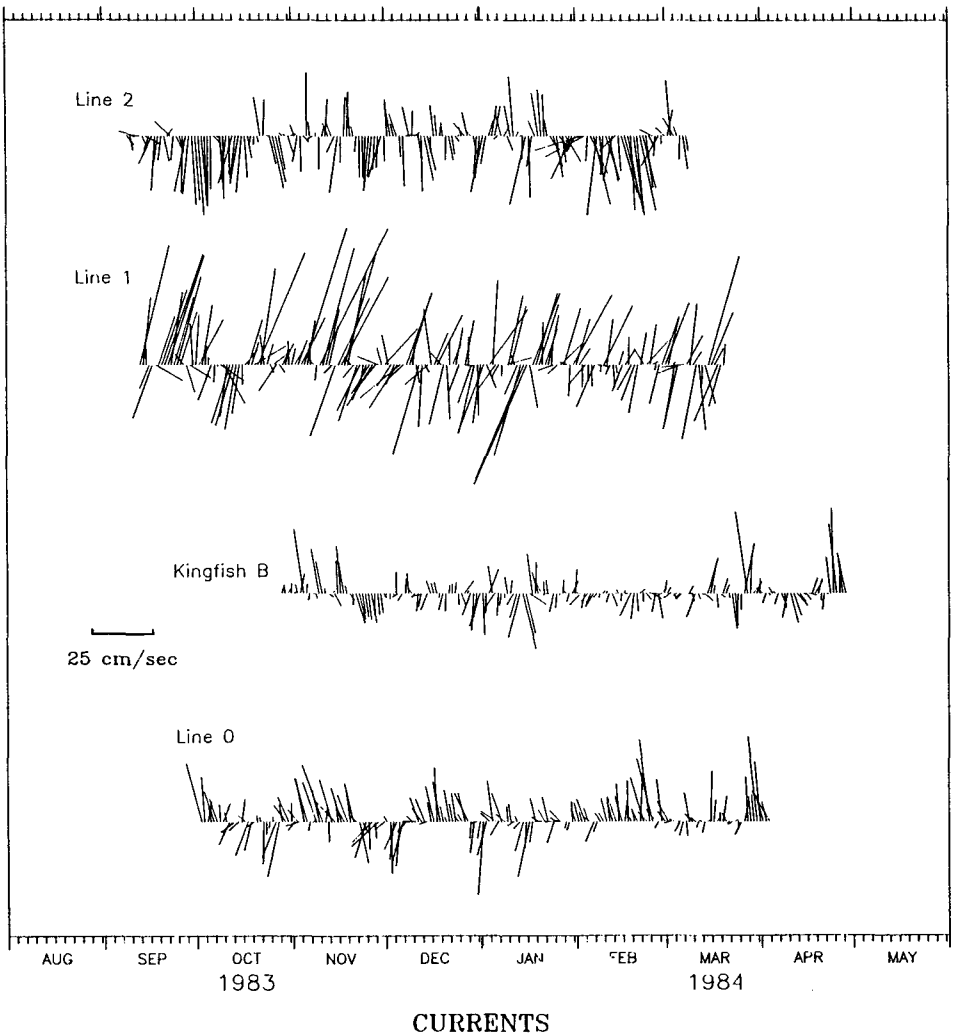

FIG. 3. Time series of low-passed current vectors from ACE (Line 0, 1, 2) and Kingfish B. The representative current record for each line used in the analysis is presented. The local alongshore component is directed toward the top of the page.

(Table 1). The currents are rotated with their alongshore components directed to the top of the page, and are basically rectilinear so only the alongshore component is considered for the analysis. All current records at each Line were rotated to the Line's mean principal axis; the currents shown for the inner mooring at Line 1 appear "tilted" relative to the principal axis defined for that Line. In the statistical analyses we use the alongshore component of wind stress and currents at each site.

3. Correlation analysis

Correlations and lagged correlations were performed on all the series, over a four month period beginning 31 October 1983. The correlations in Table 2 are based on six hourly data to determine the shorter lags between closely spaced stations. The propagation speed is also estimated, eastward through Bass Strait and northward along the east Australian coast. The average time scale of the wind and the current is approximately 1.6 and 1.8 days, respectively; yielding 70 degrees of freedom over the 124 days analysed.

The current correlations in Table 2 show a maximum between the KFB and Line 1 currents (0.88), with KFB leading Line 1 currents by 0.5 days (propagation speed of 4.2 m s^{-1}). This gives the same propagation speed as on the east Australian coast, where Line 1 currents lead Line 2 currents by one day (correlation 0.64; propagation speed 4.4 m s^{-1}). The maximum correlation between currents at KFB and Line 0 (to the east of Tasmania) is less (0.51). The implied propagation speed of greater than 12 m s^{-1} is both unrealistically fast and in the wrong direction for a coastal trapped wave response.

The wind stress correlations are highest between KFB and Line 1 (Gabo Island, 0.77) with a 0.25 day lag; the correlations decrease with distance along the coast. The correlation between wind stress at Gabo Island and Wollongong is high (0.65) but again is maximum at a near zero lag, implying a fast propagation speed. These results are from a four month summer period and correspond to weather systems moving in an eastward direction across southern Australia and Bass Strait, with fronts moving rapidly northward up the inclined east coast of Australia with an average speed of 11.5 m s^{-1} (Baines 1980).

The correlations for the alongshore component of current and the alongshore wind stress give some indication of the wind forcing (Table 2). The currents at KFB and Line 1 are highly correlated with the winds at Kingfish B; both show a correlation of 0.85 but the lags of 0.25 days and 0.75 days respectively implying propagation. The currents at Line 1 are slightly better correlated with KFB winds than with their local winds at Gabo Island (0.76), but the difference is not statistically significant. However the pattern is consistent with the results of Halliwell and Allen (1984) who found that forced fluctuations in sea level, which propagated poleward along the west coast of North America, showed a higher correlation with winds measured earlier and equatorward than with the local winds. These

TABLE 2. Correlations and lagged correlations for alongshore wind stress (τ^y) and alongshore currents (v). The period of analysis covers 121 days beginning 31 October 1983. The 99% significance level is <0.44 for all pairs. The implied propagation speed is in m s^{-1} and is positive eastward through Bass Strait and positive northward (equatorward) along the east Australian coast. The maximum correlation is obtained when the second series lags the first by the time indicated.

Series 1	Series 2	Separation (km)	Zero lag correlation	Max lag correlation	Lag (days)	Propagation speed (m s^{-1})
			Bass Strait results			
KFB τ^y	vs Line 1 τ^y	160.	0.73	0.77	.25	7.4
	Line 2 τ^y	530.	0.58	0.67	.5	12.2
	vs KFB v	0.	0.83	0.85	.25	—
	Line 0 v	−525.	0.42	0.60	.75	—
	Line 1 v	180.	0.57	0.85	.75	—
	Line 2 v	560.	0.06	0.57	1.75	—
KFB v	vs Line 0 v	−525.	0.44	0.51	.5	−12.2
	Line 1 v	180.	0.74	0.88	.5	4.2
	Line 2 v	560.	0.15	0.60	1.75	3.7
			ACE results			
Line 1 τ^y (Gabo)	vs Line 2 τ^y	370.	0.66	0.66	0.	—
	vs Line 0 v	−620.	0.49	0.49	0.	—
	Line 1 v	20.	0.68	0.76	0.25	—
	Line 2 v	400.	0.17	0.72	1.5	—
Line 1 v	vs Line 0 v	−705.	0.53	0.53	0.	—

correlations and lags confirm that the winds and currents in the region from KFB to Line 1 are strongly linked.

We wish to consider whether the currents at KFB are correlated with the currents attributed to CTWs at Lines 1 and 2. To do this we compare the currents at KFB with the modeled dynamic modes calculated from the ACE dataset (Church et al. 1986a; Huyer et al. 1988). The dynamic modes are the result of decomposing the current fluctuations into three coastal trapped wave modes and one eddy mode, and provide a model of coastal trapped waves off the east Australian coast. The "Eddy" mode represents the variance within the current record that is due to the eddies from the East Australian Current impinging on the shelf. The ACE analysis shows that most of the energy is represented by the first two dynamic modes.

Table 3 shows the correlations between KFB currents and the four dynamic modes. The correlation between Kingfish B currents and Line 1 currents (0.88) was higher than for the individual dynamic modes. The currents at KFB have a higher correlation with the second dynamic mode at Line 1 (0.78) than with the first dynamic mode (0.68). This is consistent with the ACE results that more Line 1 energy was explained by Mode 2 (49%) than Mode 1 (30.5%) (Church et al. 1986a). The Line 2 dynamic modes showed a lower correlation with the Kingfish B currents, being further from the forcing region. These correlations suggest the first two coastal trapped waves modes may originate in Bass Strait. The correlation between KFB winds and the dynamic modes show similar results, as expected from the high correlation between KFB winds and currents.

4. Spectral analysis

For a detailed view of the frequency dependence between alongshore currents and the Bass Strait or local wind stress forcing, we have computed the cross-spectra between currents and wind stress at various locations along the east Australian coast. The spectra are calculated over the longest common period between all the datasets, 124 days from 31 October 1983 to 3 March 1984, which roughly corresponds to the "eddy-free" period described for the ACE Experiment (Huyer et al. 1988). All cross-spectra are calculated with a bandwidth spanning five frequencies, giving ten degrees of freedom.

The auto- and cross-spectra between the alongshore currents at KFB and the three ACE current records are shown in Fig. 4a. The currents at Line 1 have the highest spectral density, whereas the currents at KFB are nearly an order of magnitude less. All the currents at KFB, Line 1 and Line 2 show a spectral peak around 0.11–0.15 cpd, which corresponds to the frequency band that consistently showed clear evidence for CTWs in the ACE dataset. Line 0 shows a different trend in the low-frequency band < 0.3 cpd, with a drop in energy in the 0.11–0.15 cpd band but with a peak in spectral density around 0.225 cpd.

The cross-spectral phase shows KFB currents leading Line 0 currents, which confirms that the currents do not propagate north from Tasmania across the escarpment in eastern Bass Strait. There is a slight coherence at 0.13 cpd but the strongest coherence between KFB and Line 0 currents occurs at 0.25 cpd. This corresponds to a secondary peak, noted in the modal structure (Mode 3) from ACE (Church et al. 1986a) and also as a strong peak in the wind spectra at all stations (Fig. 4b). It is likely that the winds in Bass Strait are part of the large scale atmospheric systems which also directly affect the currents off eastern Tasmania.

The alongshore component of currents at KFB and Line 1 were highly coherent at all frequencies. Current fluctuations are observed to propagate from KFB to

TABLE 3. Correlations and lagged correlations for alongshore current at Kingfish B with the dynamical orthogonal modes from the ACE analysis. The period of analysis covers 121 days beginning 31 October 1983. The 99% significance level is <0.44 for all pairs. The maximum correlation is obtained when the second series lags the first by the time indicated..

Series 1	Series 2	Zero lag correlation	Maximum lag correlation	Lag (days)	Propagation speed (m s^{-1})
		Line 1			
KFB v	vs Dyn mode 1	0.56	0.68	0.5	4.2
	Dyn mode 2	0.65	0.78	0.5	4.2
	Dyn mode 3	0.13	0.38	1.5	—
	Dyn eddy	−0.16	−0.28	2.0	—
	vs Line 1 v	0.74	0.88	0.5	4.2
		Line 2			
KFB v	vs Dyn mode 1	0.05	0.45	2.0	3.2
	Dyn mode 2	0.10	0.44	2.0	3.2
	Dyn mode 3	0.11	0.30	10.0	—
	Dyn eddy	−0.19	−0.24	31.5	—
	vs Line 2 v	0.15	0.60	2.0	3.2

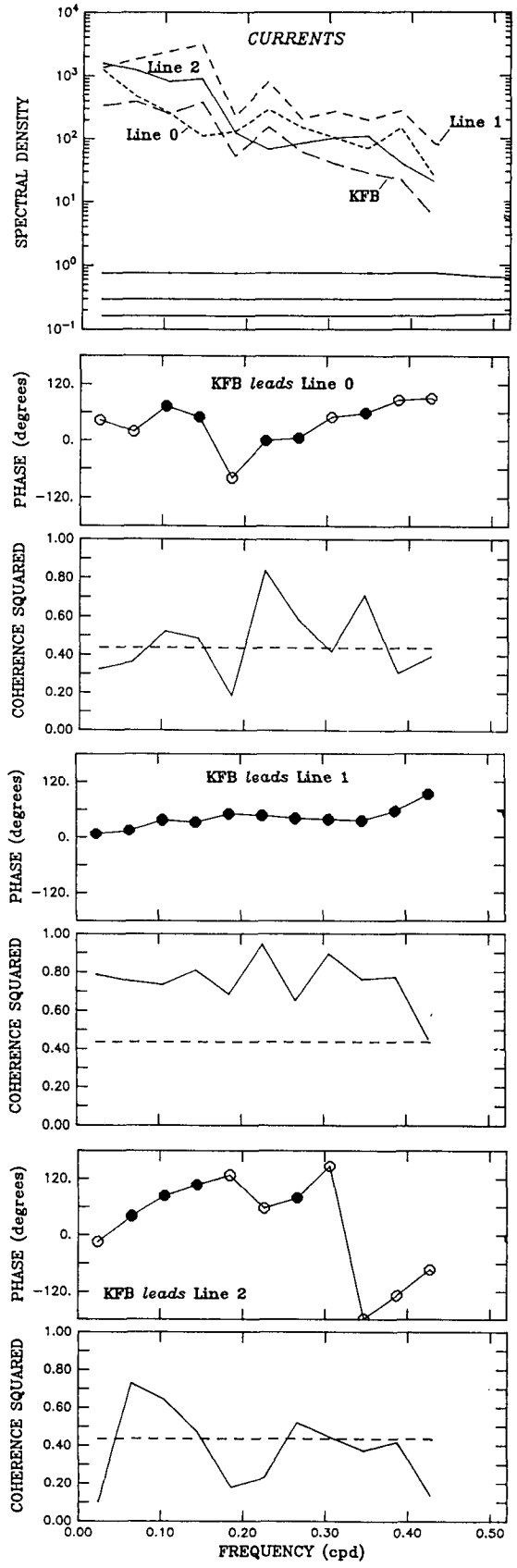

FIG. 4a. Autospectra and cross spectra between alongshore components of current. In each column the panels (top to bottom) show spectral density in $(\text{cm s}^{-1})^2/\text{cpd}$ and the phase and coherence between KFB data and the ACE data. The 90% confidence limits are shown.

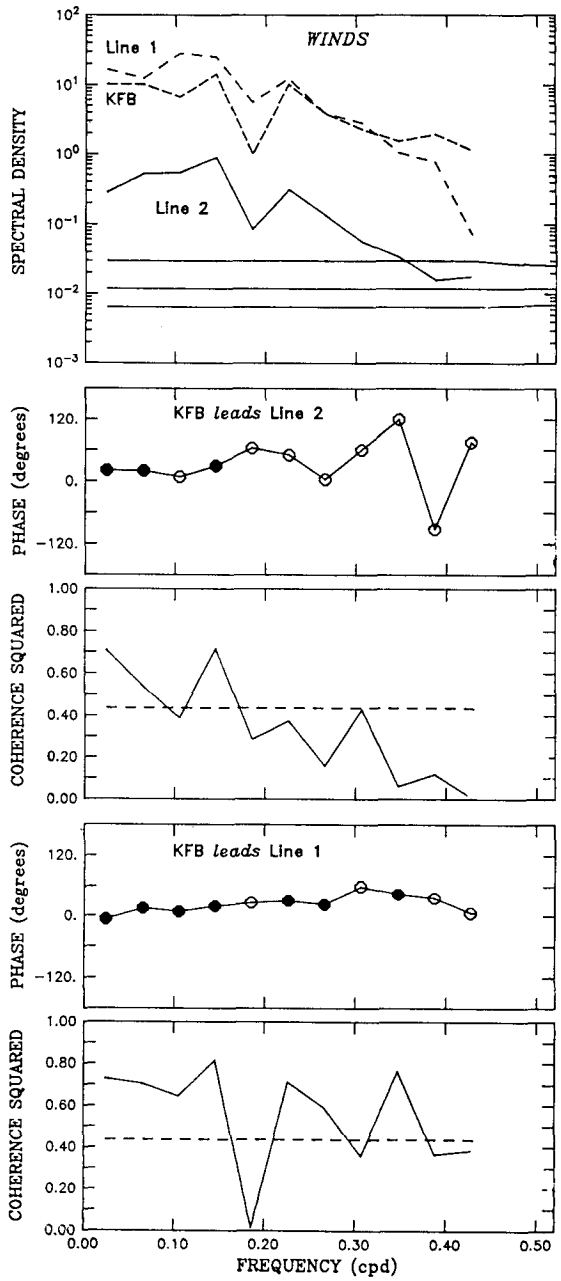

FIG. 4b. Autospectra and cross spectra between alongshore components of wind stress. In each column the panels (top to bottom) show spectral density in $(\text{dyn cm}^{-2})^2/\text{cpd}$ and the phase and coherence between KFB data and the ACE data. The 90% confidence limits are shown.

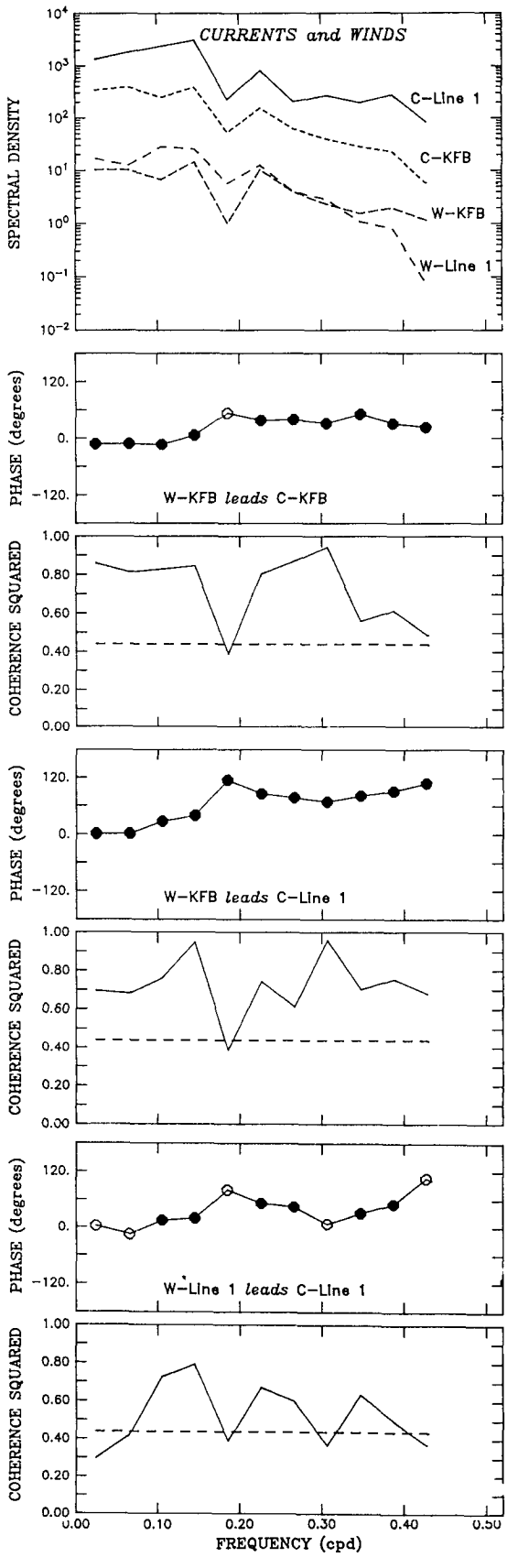

Line 1 at a phase speed of 3.1 m s^{-1}, the same as the first mode phase velocity from Line 1 to Line 2 in the ACE analysis (3.2 m s^{-1}, Church et al. 1986a). KFB and Line 2 are also coherent in the low-frequency band of 0.06–0.14 cpd, and again the phase propagates at 3.1 m s^{-1}.

The spectra of the alongshore component of wind stress at each station are shown in Figure 4b. The KFB and Gabo Island series are coherent over a larger frequency range, but again 0.13 cpd gives a maximum coherence. There is a drop in wind energy at all locations around 0.18 cpd (5.5 days). This gap in energy is probably a result of the different scale storms that pass through the region. It is interesting to note that this decrease in energy also appears in the current spectra. There is a secondary peak in wind and current energy around 0.225 cpd that shows significant coherence, especially at locations near Bass Strait. The phase speeds in current and wind at this frequency are similar to the 0.13 cpd results (Figs. 4a,b).

The relationship between wind stress and currents at KFB and Line 1 is illustrated by auto and cross-spectra (Fig. 4c). The peak in wind energy at 0.13 cpd and the trough at 0.18 cpd are also evident in the current spectra at KFB and Line 1. The high coherences in the cross-spectra confirm that the currents at KFB and Line 1 are strongly influenced by the wind regime in eastern Bass Strait. The KFB currents are highly coherent with the local KFB winds, except at the energy minimum at 0.18 cpd.

Indeed the currents at Line 1 are more coherent with KFB wind stress than with their local (Gabo Island) wind stress, though again the difference is not statistically significant. In Bass Strait the effective wind stresses are from the large-scale weather systems, affecting both Bass Strait proper and the adjacent waters. The wind-driven currents from eastern Bass Strait may be further forced by the wind stress in the region between KFB and Line 1; so the Line 1 currents carry the signature of Bass Strait currents with additional "local" wind forcing.

It is useful to examine the alongshore distributions of coherence and phase of all the wind and current stations. Figure 5 shows the coherence and phase between the Kingfish B wind stress record and each of the wind and current records along the coast. The results for 0.137 cpd are presented—the frequency which consistently showed the highest coherences in all the wind and current records. The data locations are plotted relative to KFB, with distances either measured alongshore (the curved path of the 200 m isobath) or

FIG. 4c. Autospectra and cross spectra between alongshore components of winds and currents. In each column the panels (top to bottom) show spectral density and the phase and coherence between KFB data and the ACE data. Spectral density is in $(\text{dyn cm}^{-2})^2/\text{cpd}$ for the winds, $(\text{cm s}^{-1})^2/\text{cpd}$ for the currents. The 90% confidence limits are shown.

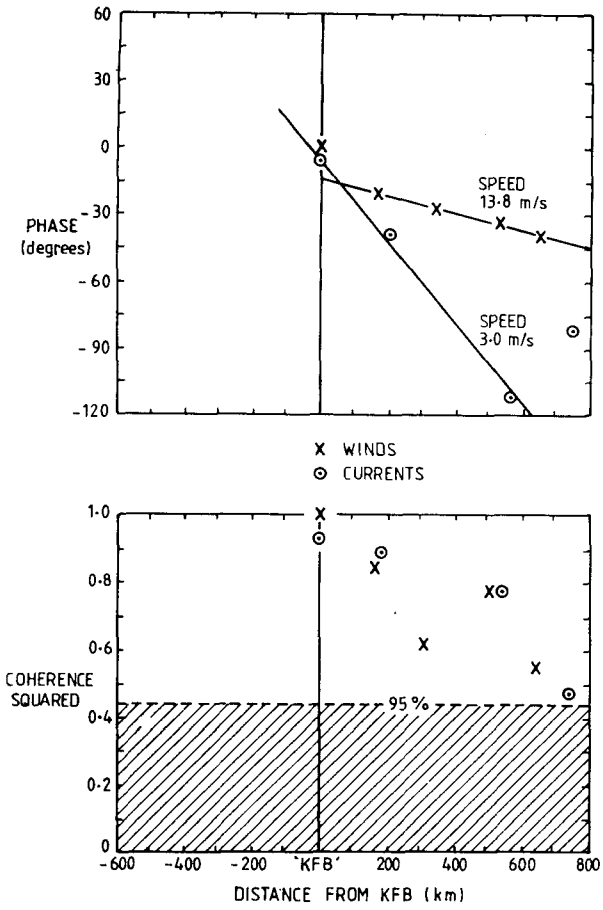

FIG. 5. Phase and coherence of alongshore wind stress and alongshore currents from the cross-spectral analysis, plotted relative to Kingfish B wind stress. Results are calculated for the frequency 0.137 cpd. Distances are measured along the 200 m isobath from Kingfish B: negative distances are westward/southward from Kingfish B; positive distances are eastward/northward.

in a straight line along Bass Strait. Negative distances are westward/southward of KFB; positive distances are eastward/northward. The phase relation between wind stress at KFB and currents (downstream in the CTW sense) follow the phase relation expected for CTWs and not the phase relationship mirroring the local winds. This strongly suggests the signal is propagating away from a generating source of CTWs near Bass Strait. The small phase difference between KFB winds and currents suggests the generation is near KFB.

5. Comparison with model and flux estimates

The Clarke (1987) model calculates the eastward energy flux at the eastern end of Bass Strait assuming that all of the flux is generated by winds within Bass Strait. The solution is the sum of two wind-forced barotropic Kelvin waves in a constant depth channel: one generated primarily on the northern coast and propagating eastward, the other generated on the southern coast with westward propagation. The Kelvin waves are modified by the wind because the wind-induced Ekman transport toward (or away from) the coast is locally determined and will build up (or reduce) the Kelvin wave. The governing equations are the same as for storm surges. The time-averaged energy flux at the eastern end of Bass Strait has the form

$$\text{flux} = \frac{h_0 g^2 \rho_0}{4f} (|\Phi(x, 0, t)|^2 - |\Phi(x, d, t)|^2)$$

where x is measured along Bass Strait, d is the width of Bass Strait, h_0 is constant depth, g is acceleration due to gravity, ρ_0 is water density, f is Coriolis parameter and each Kelvin wave $\Phi(x, y, t)$ has the form:

$$\Phi(x, y, t) = A(x) \exp(i\omega t + \alpha y) + B(x) \exp(i\omega t - \alpha y).$$

Here $A(x)$ and $B(x)$ are functions of wind stress and the boundary conditions. For full details of the model refer to Clarke (1987). It is important to note that the time-averaged energy flux is based on the fourth power of wind speed, or the wind stress squared. So small changes in wind speed have a large effect on energy flux.

We can determine the alongshore current and associated energy flux at the eastern end of Bass Strait, by applying the known wind stress for Bass Strait to the Clarke (1987) model (Table 4). The energy flux calculations are strongly dependent on the wind stress estimates. For example the standard deviation of Gabo Island wind stress (0.31 N m^{-2}) applied by Clarke (1987) gives an energy flux of 1.96×10^8 W, 10% larger than the flux entering Line 1. If the wind stress from KFB (0.23 N m^{-2}) is assumed appropriate for the whole of Bass Strait (since it clearly is the most representative of the stress over the water), the calculated energy flux is 1.08×10^8 W, or 60% of the measured energy flux at Line 1.

We had earlier noted that Freeland et al. (1986) and Church et al. (1986a) had estimated the energy flux for coastal trapped waves traveling between eastern Bass Strait and Cape Howe. Assuming the same coupling coefficients in the CTW equations that were appropriate for Cape Howe will also apply in eastern Bass Strait, they estimated the wind-driven energy flux in this region to be about 20% of the total flux entering Line 1. The total energy flux at Line 1 should be a sum of the energy flux generated within Bass Strait, e.g., from the Clarke (1987) model, and the wind-driven energy flux generated east of the Strait, providing 80% of the measured energy flux at Line 1.

To test the energy flux model we compared the results with data from eastern Bass Strait. The modeled barotropic wind-driven Kelvin waves have amplitudes of O (4–13 cm) at the coast, with associated alongshore currents of only O (1–3 cm s^{-1}). The standard deviation of the observed sea level at Lakes Entrance in east-

TABLE 4. Model estimates of alongshore current (v) and energy flux at the eastern end of Bass Strait, for varying wind stress estimates. Calculated following Clarke (1987) model for wind-driven Kelvin waves in Bass Strait. The standard deviation of observed alongshore current at KFB is 12 cm s^{-1}.

Wind stress		Kelvin wave			
Site	Std. dev. (N m^{-2})	Amplitude at coast (cm)	Alongshore current (cm s^{-1})	Energy flux ($\times 10^8$ W)	Percent flux at line 1 (%)
Gabo Island	0.31	10.9	2.6	1.96	110.*
KFB (10 m)	0.23	8.1	2.0	1.08	60.
KFB (65 m)	0.37	13.0	3.2	2.79	155.

Period = 8 days
* Estimate used in Clarke (1987).

ern Bass Strait (13 cm; Church and Freeland; 1987) is comparable to the model results. However the Kelvin wave model predicts only 16% of the standard deviation of current at KFB. This is not surprising as the location is close to the shelf break and the flow should be gaining more "shelf wave" characteristics (larger currents and lower sea level amplitudes) than the modeled channel flow.

Although the model underestimates the observed flux at Line 1, one should keep in mind that the example used in Clarke (1987) assumes Bass Strait is a constant 80 m depth and constant width. However the average depth varies, depending on how the model length and width is defined. Clarke (1987) estimates that if a water depth of 60 m is assumed (as in Freeland et al. 1986) the energy flux will be increased by 30%, to provide almost all the energy flux entering at Line 1.

6. Discussion and summary

Our analysis of the wind and current records at KFB, in conjunction with the ACE results, has supported the idea that the coastal trapped wave energy which enters the ACE region at Cape Howe is propagating from Bass Strait.

At KFB, the winds and currents were found to be highly coherent and almost in phase, with currents lagging the wind by 12.5 degrees. This is consistent with local wind forcing (Jones 1980). The wind field is spatially uniform and remains highly coherent between KFB and Line 1. Since the current is also coherent between the two sites, the phase information allows us to determine the probable origin of wind forcing.

At KFB the wind and current are almost in phase but by Line 1 the current phase lags the wind. As Fig. 5 shows, the currents and wind have different phase speeds between KFB and Line 1; the currents propagate at 3.1 m s^{-1} while the wind phase speed is 6–10 m s^{-1}. At a frequency of 0.38 cpd the wind has become 90° out of phase with the current. Since the wind and the current do not remain in phase between KFB and Line 1, we can assert that most of the forcing occurs in Bass Strait.

The energy flux from wind forcing over Bass Strait was investigated by applying the high-quality KFB winds to the Clarke (1987) model. The resultant energy flux at the eastern end of Bass Strait was 60% of the total energy measured entering Line 1. However, if we add to this the Freeland et al. (1986) and Church et al. (1986a) estimates for wind driven energy flux between eastern Bass Strait and Line 1 we get a total energy flux which is about 80% of the observed flux entering at Line 1. Recall also the model assumes Bass Strait to have a constant depth of 80 m. If a 60 m depth is applied (which is not unreasonable—see Fig. 1) the strait energy flux is increased by 30%. Given the uncertainties of the model these results are consistent with the theory that most of the energy flux entering the ACE region is generated in Bass Strait.

The standard deviation of velocity at KFB is larger than that predicted by a Kelvin wave model for Bass Strait, but smaller than the Line 1 velocity. This reflects the positioning of KFB at the shelf break, where the flow is gaining more "shelf characteristics" than the modeled channel flow.

There may be additional wind forcing of the currents in the region between KFB and Line 1. Lopez and Clarke (1989) consider a "local plus remote" (LPR) solution for CTWs. The first dynamic modes are driven by remote forcing that depends on non-local wind stress and the higher order modes are effectively generated by the local wind. Our results support this concept as the first two dynamic modes at Line 1 show a higher correlation with KFB winds than with the local winds. The additional local forcing must be a small portion of the total variance: Freeland et al., (1986) estimate only 20% of the velocity variance of CTWs at Line 1 is locally forced. However the local forcing may explain the subtle differences in variance, phase speed and energy flux in the ACE array.

It is possible that some additional energy flux could propagate in some form from the Great Australian Bight. Clarke (1987) has applied boundary conditions in his model that allow no energy to enter the western and eastern ends of Bass Strait. However Church and Freeland (1987) have indicated that Bass Strait may be a sink to smaller wavelength CTW energy propa-

gating from the west, although how it propagates across Bass Strait has not been determined.

It appears that the eastern Bass Strait region is an important area of change, where energy from Bass Strait, possibly in the form of the wind-driven barotropic Kelvin wave discussed by Clarke (1987), is transferred to coastal trapped waves. There is insufficient cross-shelf data at KFB to determine an accurate modal structure of possible CTWs at this location. More information is required in this region before we can test how energy from Bass Strait is transferred into CTW energy at Line 1.

Acknowledgments. We would like to thank ESSO/BHP for access to their oil and gas platforms for oceanographic research over the last ten years. We also wish to acknowledge the financial assistance of the RAN Research Laboratory and the MST Grants Scheme. Partial support for ACE and for the analysis in this paper came from the U.S. Office of Naval Research and the U.S. National Science Foundation.

REFERENCES

Baines, P. G., 1980: The dynamics of the Southerly Buster. *Aust. Meteor. Mag.* **28**(4), 175–200.

Buchwald, V. T., and B. J. Kachoyan, 1987: Shelf waves generated by a coastal flux. *Aust. J. Mar. Freshwater Res.*, **38,** 429–437.

Church, J. A., and H. J. Freeland, 1987: The energy source for the coastal-trapped waves in the Australian Coastal Experiment region. *J. Phys. Oceanogr.*, **17,** 289–300.

——, ——, and R. L. Smith, 1986a: Coastal-trapped waves on the east Australian continental shelf. Part I: Propagation of modes. *J. Phys. Oceanogr.*, **16,** 1929–1943.

——, N. J. White, A. J. Clarke, H. J. Freeland and R. L. Smith, 1986b: Coastal-trapped waves on the east Australian continental shelf. Part II: Model verification. *J. Phys. Oceanogr.*, **16,** 1945–1957.

Clarke, A. J., 1987: The origin of the Australian Coastal Experiment coastally trapped waves. *J. Phys. Oceanogr.*, **17,** 1847–1859.

——, and R. O. R. Y. Thompson, 1984: Large-scale wind-driven ocean response in the Australian Coastal Experiment region. *J. Phys. Oceanogr.*, **14,** 338–352.

——, and S. Van Gorder, 1986: A method of estimating wind driven shelf and slope water flow. *J. Phys. Oceanogr.*, **16,** 1011–1026.

Forbes, A. M. G., 1987: Wind stress in the Australian Coastal Experiment region. *Aust. J. Mar. Freshwater Res.*, **38,** 475–489.

Freeland, H. J., J. A. Church, R. L. Smith and F. M. Boland, 1985: Current meter data from the Australian Coastal Experiment; a data report. CSIRO Marine Laboratories Rep. No. 169.

——, F. M. Boland, J. A. Church, A. J. Clarke, A. M. G. Forbes, A. Huyer, R. L. Smith, R. O. R. Y. Thompson and N. J. White, 1986: The Australian Coastal Experiment: A search for coastal trapped waves. *J. Phys. Oceanogr.*, **16,** 1230–1249.

Gill, A. E., and A. J. Clarke, 1974: Wind-induced upwelling, coastal currents and sea-level changes. *Deep-Sea Res.*, **21,** 325–345.

Halliwell, G. R., and J. S. Allen, 1984: Large-scale sea level response to atmospheric forcing along the west coast of North America, summer 1973. *J. Phys. Oceanogr.*, **14,** 864–886.

Hamon, B. V., 1962: The spectrums of mean sea level at Sydney, Coff's Harbour and Lord Howe Island. *J. Geophys. Res.*, **67,** 5147–5155. [Correction, 1963, *J. Geophys Res.*, **68**(15), 4635.]

——, 1966: Continental shelf waves and the effects of atmospheric pressure and wind stress on sea level. *J. Geophys. Res.*, **71,** 2883–2893.

Huyer, A., R. L. Smith, P. J. Stabeno, J. A. Church and N. J. White, 1988: Currents off southeastern Australia: Results from the Australian Coastal Experiment. *Aust. J. Mar. Freshwater Res.*, **39,** 245–288.

Jones, I. S. F., 1980: Tidal and wind-driven currents in Bass Strait. *Aust. J. Mar. Freshwater Res.*, **31,** 109–177.

Large, W. S., and S. Pond, 1981: Open ocean momentum flux measurements in moderate to strong winds. *J. Phys. Oceanogr.*, **11,** 324–336.

Lopez, M., and A. J. Clarke, 1989: The wind-driven shelf and slope water flow in terms of a local and a remote response. *J. Phys. Oceanogr.*, **19,** 1091–1101.

Wu, J., 1980: Wind-stress coefficients over sea-surface near neutral conditions—a revisit. *J. Phys. Oceanogr.*, **10,** 727–740.